RSC Advances

ROYAL SOCIETY OF CHEMISTRY

www.rsc.org/advances

Study of N-Benzylidene derivatives synthesized as corrosion inhibitors for copper in HCl solution

Mohsen Behpour [a,*], Mehdi Shabani-Nooshabadi [a], Faezeh Sadat Razavi [a], Masood Hamadanian [b,c], Vajihe Nejadshafiee [a]

[a] *Department of Analytical Chemistry, Faculty of Chemistry, University of Kashan, Kashan, P.O. Box 87317-51167, I.R. Iran*

[b] *Institute of Nanosciences and Nanotechnology, University of Kashan, Kashan, Iran*

[c] *Department of Physical Chemistry, Faculty of Chemistry, University of Kashan, Kashan, Iran*

E-mail: m.behpour@kashanu.ac.ir

* corresponding author:
E-mail address: m.behpour@kashanu.ac.ir
Fax No: +983155912935, Tel No:+983155912930

Abstract

Corrosion inhibition of the two N- Benzylidene derivative compounds, namely N-benzylidene Pyridin – 2 amine (NBPA) and N-(4-choloromethylbenzylidene) Pyridin – 2 amine (NCMBPA) as corrosion inhibitors for copper in hydrochloric acid 6.0 M have been studied by electrochemical methods such as potentiodynamic polarization measurements and electrochemical impedance spectroscopy. Potentiodynamic polarization results show that corrosion potentials shift to anodic regions in the presence of N- Benzylidene compounds compared to blank solution. The electrochemical measurements indicated that the inhibition efficiency for NCMBPA about 92% and NBPA about 85%**.** The adsorption of inhibitors on the copper surface follows from Langmuir adsorption isotherm. Activation energy (E_a), Gibbs free energy (ΔG_{ads}), enthalpy (ΔH^*), and entropy (ΔS^*) of corrosion process are determined by using the experimental measurements.

Keywords: Acid inhibition; Corrosion; Copper; Impedance spectroscopy; Polarization

1. Introduction

Copper and its alloys are extensively applied in many fields on account of their electrical, thermal and mechanical properties such as ductility, hardness, strength and low price. Safety of copper is of exacting interest, particularly in acidic media, which also includes chloride ions[1-6].

Copper is susceptible against corrosion in such separate surroundings, although it is highly resistant in practically neutral or slightly alkaline aqueous environment. The utilization of suitable inhibitor to offer an explanation the particular corrosion mechanism of copper in acidic chloride environments is essential. It is commonly accepted that anodic dissolution of copper in chloride environments is influenced by the chloride concentration and the acidity of the medium. At chloride

concentrations lower than 1.0 M, the dissolution of copper occurs through formation of CuCl which is not defensive enough and is changed to the soluble $CuCl_2^-$ by reacting with excess chloride. Alternatively, at concentrations higher than 1.0 M, higher copper complexes such as $CuCl_3^{-2}$ and $CuCl_4^{-3}$are formed, in addition to the ones with fewer chlorides, such as CuCl and $CuCl_2^-$ [7].

Most of acid corrosion inhibitors are organic compounds containing electronegative atoms (such as, N, S, P, O, etc.), the unsaturated bounds (such as, double bonds or triple bonds, etc.) and the plane conjugated systems containing all kinds of aromatic cycles [8-13]. The inhibiting action of these compounds is usually attributed to their interactions with copper surface by their adsorption [14-16].The usage of nitrogen and sulfur containing organic compounds as corrosion inhibitor for copper has been commonly investigated [17-27]. Some Schiff bases have been recently studied as corrosion inhibitors for different metals and alloys in acid media [28–32]. These materials usually become effective by adsorption on the metal surface. The adsorbed species protect the metal from the aggressive medium, which causes decay of the metal. Adsorption depends on not only the nature and charge of the metal but also on the chemical structure of the inhibitor.

Increasing popularity of Schiff bases in the field of corrosion inhibition science based on the ease of synthesis from relatively inexpensive starting materials and their eco-friendly or low toxic properties [33, 34]. The high inhibitory performance of these compounds results from the substitution of different heteroatoms (N, O, Cl and Br) and π-electrons in their structure in besides the presence of imine (—C=N—) functional group [35, 36]. This organic compound having general formula R–C=N–R' where R and R' are aryl, alkyl or cycloalkyl or heterocyclic groups formed by the condensation of an amine and a carbonyl group, is a potential inhibitor. These molecules normally form a very thin and persistent adsorbed film that lead to decrease in the corrosion rate due to the slowing down of

cathodic, anodic reaction or both [37–39]. In order to improve the inhibitive force, synergistic inhibition effect is an effective method [40].

In the present work, the inhibition effect of NBPA and NCMBPA on the corrosion of copper in 6.0 M HCl solution was firstly investigated by potentiodynamic polarization curves, electrochemical impedance spectroscopy (EIS). The adsorption isotherm and adsorption free energy were found and discussed. Effects of inhibitor concentration, temperature on the corrosion inhibition were fully investigated. Quantum chemical calculation of including the solvent effect is applied to study the difference in theoretical parameters between neutral inhibitor molecule and protonated inhibitor molecule. It is estimated to collect useful information on the inhibition effect of NBPA and NCMBPA on copper corrosion in HCl solution.

2. Experimental

2.1. Material

2.1.1. General procedure for the synthesis of Schiff base ligands

All the di dentate Schiff base ligands were prepared by condensation between aldehyde and pyridine-2-amine in ethanol (EtOH) and purified by recrystallization from ethanol through the partial evaporation of the more volatile dichloromethane. Schiff base ligands prepared by dissolving aldehyde (1 mmol) and pyridine-2-amine (1 mmol) in ethanol with stirring in one portion. The stirring was continued to completion of the reaction. The progress of the reaction was monitored by thin layer chromatography (TLC). After the completion of the reaction, a colored substance was obtained. The solid product was filtered and washed with cold EtOH. The crude product was purified by recrystallization from ethanol and the pure Schiff base was obtained in high yield after leaving for the appropriate time (Fig 1) [41].

2.1.2. Solutions and samples

The corrosive solution is prepared by dilution of analytical grade hydrochloric acid 11.0 M with double distilled water. The concentration range of employed inhibitors is 0.01 to 0.0005 M in 6.0 M HCl.

The metal of this study was copper having 99.9% purity. Copper panels were rectangular in size (1.0 cm, 1.0 cm, 0.1 cm). The panels were soldered with Cu-wire for electrical connection and mounted into the epoxy resin to offer only one active flat surface exposed to the corrosive environment. Prepare panels incorporated abrasion with SiC abrasive paper 400-2500 grades. The above samples were ultrasonically cleaned with ethanol and double distilled water, respectively. Then, they were dried at room temperature before immersion in experimental solution.

2.2. Electrochemical measurement

Electrochemical studies were carried out using an AUTOLAB model PGSTAT 30. The usual three electrode system was used for this purpose. Copper specimen was used as a working electrode. Pt electrode and silver-silver chloride Ag/AgCl (3.0 M Cl^-) served as counter and reference electrodes, respectively. All polarization and impedance curves were recorded at room temperature (25±2 ^{0}C). The working electrode was immersed in the test solution for 1000 seconds until a steady state open-circuit potential was attained. NOVA software was used for fitting impedance data in an equivalent circuit as well as for extrapolating Tafel slopes. Experiments were carried out in triplicate to ensure reproducibility of results.

2.3. Electrochemical impedance spectroscopy study

The EIS measurements were performed over the frequency range 100 kHz to 100 mHz at the open circuit potential by superimposing alternating current (AC) signal of 0.01V after immersion for 1000 second in the corrosive media. The inhibition efficiencies for each inhibitor concentration were calculated using the eq 1:

$$\eta\% = \frac{R_{ct} - R_0}{R_{ct}} \times 100 \quad (1)$$

where R_{ct} and R_0 are the charge transfer resistances in the presence and absence of the inhibitor respectively.

2.4. Potentiodynamic polarization

The potentiodynamic polarization curves were recorded from -200 to 200 mV (vs. Ag/AgCl (3.0 M Cl^-)) corresponding to the corrosion potential with scan rate of 0.01 mV s^{-1}. The inhibition efficiencies at different inhibitor concentrations were estimated using the eq 2:

$$\eta\% = \frac{i_0 - i_1}{i_0} \times 100 \quad (2)$$

where i_0 and i_1 are the corrosion current densities in the absence and presence of the inhibitor, respectively.

2.5. Quantum chemical study

All the calculations were performed with of complete geometry optimization by using the standard Gaussian 98 software package with semi-empirical methods including the Austin Model B3LYP with 6-311G** basis set and Conductor-like Screening Model' or COSMO method which includes PCM and CPCM methods[42]. COSMO is a calculation method for determining the electrostatic interaction of a molecule with a solvent. The polarizable continuum model (PCM) is a commonly used method in computational chemistry to model solvation effects. If it were necessary to

consider each solvent molecule as a separate molecule, the computational cost of modeling a solvent-mediated chemical reaction would grow prohibitively high. Modeling the solvent as a polarizable continuum, rather than individual molecules, makes initio computation feasible. Two types of PCMs have been popularly used: dielectric PCM (D-PCM) which deals the continuum as a polarizable dielectrics and conductor-like PCM (C-PCM) which deals the continuum as a conductor-like picture similar to COSMO Solvation Model[69,70]. The molecule sketch of Schiff bases was drawn in Gauss View 3.0.

2.6. Scanning electron microscopy (SEM) studies

In order to get insight into the changes on surface of corrosive samples before and after the addition of inhibitors, the specimens were first immersed in 6.0 M HCl in the absence and presence of 0.01 M NBPA or NCMBPA for 3 h, respectively. Then taken out from the test solutions, cleaned with double-distilled water and dried at room temperature. The SEM images were conducted using a Philips scanning electronic microscope model XL30.

3. Result and discussion

3.1. Electrochemical impedance spectroscopy measurements

Fig. 2 shows the Nyquist plots of copper in a 6.0 M HCl solution in the absence and presence of NBPA and NCMBPA in different concentrations. As seen in Fig. 2. The Nyquist plots of blank solutions (hydrochloric acid 6.0 M) show Warburg impedance at low frequencies (Fig. 3) and only one depressed capacitive loop. Warburg impedance in the absence of inhibitors shows that the dissolution mechanism of copper is controlled by mass transport rate. The diffusion step of copper dissolution in several papers is ascribed to the transport of chloride ions to the surface or the transport of chloride-copper complexes43, and the depressed capacitive loop has been ascribed to roughness

and in-homogeneities on the surface during corrosion [44]. This behaviour is unchanged by the presence of the inhibitor, indicating the activation-controlled nature of the reaction throughout a one-charge transfer process. All EIS spectra were analyzed by the equivalent circuit in Fig. 3, which shows a single transfer reaction and fits well with our experimental results. R_s represents the ohmic resistance of the solution and R_{ct} represents the charge transfer resistance whose value is an estimation of electron transfer across the surface and is contrary relative to corrosion rate. The constant phase element, CPE, is introduced in the circuit instead of a pure double layer capacitor to give a more accurate fit [45]. The impedance of the CPE is expressed by the eq 3:

$$Z_{CPE} = [Y_0 (j\omega)^n]^{-1} \quad (3)$$

where Y_0 is the magnitude of the CPE, ω the angular frequency ($\omega = 2\pi f$, where f is the AC frequency), j is the imaginary unit and n the CPE exponent (phase shift). When the value of *n* is 1, the CPE behaves like an ideal double-layer capacitance (C_{dl}).

The experiments are repeated three times and fitted spectra are listed in Table 1. The data of Table 1 show that the R_s values are very small contrast to the R_{ct} values. R_{ct} is a measure of electron transfer across the surface and is inversely proportional to corrosion rate. The R_{ct} values increased with inhibitor concentrations may suggest the formation of a protective layer on the electrode surface. This layer makes a barrier for mass and charge-transfer [46]. The R_{ct} value of the blank solution is about 98.6 Ω cm^2, while the R_{ct} for NBPA inhibited solution increases to about 847.4 Ω cm^2 and for NCMBPA inhibited solution increase about 1257.8 Ω cm^2. The results show the inhibited molecules on the copper surface might be a barrier to the communication between oxide species and ionic solution.

3.2. Potentiodynamic polarization measurements

The potentiodynamic polarization curves of copper in 6.0 M HCl with and without different concentrations of NBPA and NCMBPA are shown in Fig. 4. As shown in the figures, the presence of inhibitors causes a major decrease in the corrosion current. Decrease of current densities indicates in both anodic and cathodic Tafel curves. This phenomenon indicates that both anodic metal dissolution and cathodic hydrogen evolution reaction are suppressed, meanwhile, the inhibition of these reactions is more pronounced with the increasing inhibitor concentration.

The values of corrosion potential (Ecorr), cathodic Tafel slope (bc), anodic Tafel slope (ba), corrosion current (icorr) and the inhibition efficiency (η) are given in Table 2. These values are getting by extrapolating the Tafel lines to the related corrosion potentials.

Examination of Table 2 shows that values of the corrosion current of copper in the inhibited solutions are lesser than that in the bare solution, and with the increasing concentration of Schiff's base inhibitors, the inhibition efficiency is increased. The inhibition efficiency finds from polarization experiments is created opposite the order: (NBPA) < (NCMBPA).

However, the difference of the inhibition efficiency between the two inhibitors is high, which can be featured to the difference between the structures of the two molecules. Alternatively, synergistic effect shows the increase in the efficiency of a corrosion inhibitor in the presence of a derivative species. The synergism effect has been reported due to the increased surface coverage on account of ion pair contacts between an organic cation and the halide anion. In inhibiting solution halide ion initially adsorbs on the corroding surface with making oriented dipoles and it eases the adsorption of inhibitor cations on the dipoles, consequently. Halide ions, especially Cl^- can increase the speed or inhibit the copper corrosion. The synergism among the Cl^- ions and organic inhibitors is very well shown. The purpose of protection is the protection in the presence of both the halide ion and the organic inhibitor in solution.

The inhibitor classified as cathodic or anodic type, if the displacement in E_{corr} is exceeds 85 mV with respect to E_{corr} of the blank and if the displacement in E_{corr} is below 85 mv, the inhibitor can be mixed type [47]. In the presence of NBPA and NCMBPA, the corrosion potential of copper shifted to the positive side more than 85 mV (vs. Ag/AgCl (3.0 M Cl^-)). The NBPA and NCMBPA act can be understood as anodic type inhibitors.

3.3. Adsorption isotherm

The adsorption of inhibitor molecules is one of the most important topics in corrosion researches. Its importance comes from not only due to its ability to provide structural information of the double layer but also due to the thermodynamic information can provide. There are two categories from the adsorption of organic molecules on the electrode surface. First, adsorb the molecules with keeping their chemical individuality. This interaction is rather feeble. This is a reversible type of adsorption. On the contrary, the interaction among molecule and the surface may be very strong. This phenomenon may cause a charge transfer between them and results new species form. This is the irreversible type adsorption.

Adsorption isotherms can offer the important information on the relations between the active sites on copper surface and the inhibitor molecules. The degrees of surface coverage (θ) for different concentrations of inhibitor in 6.0 M HCl solution have been calculated from the consequences of potentiodynamic polarization or EIS measurements with the eq 4 [48, 49] :

$$\theta = \frac{\eta}{100} \quad (4)$$

In this paper, with the intention of identify the nature and the strength of adsorption a series of experimental adsorption isotherms were obtained as shown in Fig 5. It is clear that all linear correlation coefficients (r) are approximately equal to 1, and the slope values are also close to 1,

which shows the adsorption of NBPA and NCMBPA on copper surface obeys Langmuir adsorption isotherm. It is represented by the eq 5:

$$\frac{C_{inh}}{\theta} = \frac{1}{K_{ads}} + C_{inh} \quad (5)$$

where C_{inh} is the concentration of inhibitor, θ is the degree of surface coverage Values for different concentrations of the inhibitors in acidic solution; respectively. That equation has been calculated with the EIS measurements.

The K_{ads} is the adsorption equilibrium constant, which is -0.85, -0.92 reveals more proficient adsorption thus better inhibition efficiency of NCMBPA on the copper surface [50]. The equilibrium constant for the adsorption - desorption process is concerned to the standard free energy of adsorption ΔG ads as said by the eq 6:

$$K_{ads} = \frac{1}{55.5} \exp\left(\frac{-\Delta G_{ads}}{RT}\right) \quad (6)$$

that R is gas constant, T is temperature in Kelvin and 55.5 is the molar concentration of water per liter solution. It is noticeable that the high value of ΔG ads turns to the best adsorption ability of organic compounds onto the metal surface. The estimated value of ΔG ads for NBPA is -33.7 kJ mol-1 and for NCMBPA is -32.6 kJ mol-1.

In general, if the values of ΔG ads are below the value of -20 kJ mol-1, they are consistent with the electrostatic interaction between the charged molecules and the charged metal (physical adsorption), while those above -40 kJ mol^{-1} are associated with chemisorption as a result of sharing or transfer of electrons from organic species to the metal surface to form a metal bond [51-53].

As mentioned in above, the calculated value for ΔG_{ads} is -33.7 kJ mol^{-1} and -32.6 kJ mol^{-1} indicating that the adsorption mechanism of NBPA and NCMBPA on copper is the chemisorption and physisorption [54].

3.4. Effect of temperature:

The study on the temperature effect of inhibition efficiency from acid-metal reaction is very difficult, for the reason that several changes take place on the metal surface, for example quick etching desorption of inhibitor and the inhibitor may undergo decomposition [55].

The effect of the temperature on the corrosion rate was studied in 6.0 M HCl both in the absence and presence of 0.01 M of the inhibitor. Consequently, the polarization analysis was carried out at different temperatures from 250C to 65 0C in the absence and presence of 0.01 M inhibitors. The electrochemical factors were extracted and summarized in Table 4. The results in Table 3 show that the corrosion (η) increases with increasing temperature in the absence and presence of inhibitor but the η increases more quickly with temperature in the uninhibited solution. It is for reason that higher temperature increases the speed of hot-movement of the organic molecules and weakens the adsorption ability of inhibitor on the metal surface [56, 57].

The energy of activation for the corrosion process was calculated from the Arrhenius equation (eq 7):

$$i_{corr} = Aexp\left(-\frac{E_a}{RT}\right) \quad (7)$$

where E_a represents apparent activation energy, R the gas constant, A is the pre-exponential factor. Values of E_a for copper in 6.0 M HCl in uninhibited and inhibited solution were estimated by linear regression between log (i_{corr}) and 1/T. The value of E_a is higher for inhibited solution (32.18 kJ mol^{-1} for NBPA, 36.86 kJ mol^{-1} for NCMBPA) than that for uninhibited solution (28.18 kJ mol^{-1}).

The high values of E_a show that more energy barrier for the corrosion reaction in the presence of the inhibitor is achieved. Therefore the adsorbed inhibitor molecules avoided charging or mass transferring from the copper surface.

The Thermodynamic parameters like enthalpy (ΔH^*) of corrosion process and entropy (ΔS^*) were calculated with the transition state eq 8:

$$C_R = \left(\frac{RT}{Nh}\right) exp\left(\frac{\Delta S^*}{R}\right) exp\left(\frac{-\Delta H^*}{RT}\right) \quad (8)$$

where h is Plank's constant and N is Avogadro's number, respectively. A plot of Ln (i_{corr} /T) vs. 1/T provides a straight line with slope = $-\Delta H^*/T$ and intercept = Ln (R/Nh) $+\Delta S^*/R$. The plots of Ln (i_{corr}/T) vs. 1/T for the corrosion of copper in the presence of different concentrations of inhibitor are shown in Fig. 6. The calculated values of activation parameters are tabulated in Table 3. The increase in activation energy (E_a) of inhibited solutions compared to the uninhibited shows that inhibitor is physically adsorbed on the corroding metal surface, while each unchanged or lower energy of activation in the presence of inhibitor shows chemisorption [58-62]. The entropy of activation in the presence and absence of the inhibitors are large and negative. Great negative values of entropies show that the activated complex in the speed determining step is connected before disconnection step indicate that a decrease in disordering happen on available from reactants to the activated complex. The positive signs of the enthalpies (ΔH^*), 25.7, 26.3 and 35.2 kJ mol^{-1} for 6.0 M HCl, NBPA and NCMBPA reflect the endothermic nature of the copper dissolution process, respectively and mean that the dissolution of copper is difficult.

3.5. Quantum chemical calculations

Quantum chemical calculations were performed in order to analyze the effect of molecular structure and also electronic parameters on present inhibitor performance. The computed quantum chemical parameters including the energy of highest occupied molecular orbital (E_{HOMO} (ev)), energy of lowest unoccupied molecular orbital (E_{LUMO} (ev)), HOMO–LUMO energy gap (ΔE(ev)) and dipole moment (μ (D)) have been presented in Table 5. According to the frontier molecular orbital theory,

the formation of a transition state is due to an interaction between the frontier orbitals (HOMO and LUMO) of reactants [63]. The HOMO is known as an orbital which could act as an electron donor because it is the outermost orbital containing electrons, having highest energy level. On the contrary, The LUMO is the innermost orbital which can accept electrons through its vacant room [64]. Basically, E_{HOMO} and E_{LUMO} are directly related to the ionization potential and the electron affinity of an organic molecule, respectively. The HOMO–LUMO gap, ΔE(ev), is an important stability index so that a large ΔE(ev) value implies high stability for the molecule in chemical reactions [65]. Inspection of Table 5 shows nearly similar value for E_{HOMO} for both compounds while NCMBPA has lower E_{LUMO}(ev) than NBPA. It may be deduced that both inhibitors have an equal ability to offer electrons to the unoccupied d-orbital of the copper, however the higher ability of accepting the electron is expected for NCMBPA in comparison with NBPA. Considering the ΔE(ev) values, the higher tendency in order to adsorb onto metal surface is measured for NCMBPA, having lower ΔE(ev) compared to NBPA. In the case of the dipole moment, it seems to be no agreement in the literature concerning the correlation between the dipole moment and the inhibition effectiveness, as yet. Since water is a polar solvent, there is a higher tendency for molecules with similar size to adsorb onto the metal surface for those who have a lower dipole moment [66]. In this study, NBPA has a lower dipole moment and molecular size in comparison with NCMBPA while both inhibitors show good inhibition efficiency. According to the above discussion, it may be concluded that both inhibitors, considering their molecular weight and dipole moment, have a tendency to adsorb onto metal surface. For instance, the higher molecular weight and dipole moment make an affinity for NCMBPA to leave the solution and get adsorbed onto surface. It should be noted that molecular electronic parameters are not confident parameters which certainly determines the corrosion inhibition performance because corrosion inhibition is a complex phenomenon.

In order to validate such correlations between calculated quantum parameters (eq 9) of experimental inhibition efficiencies for the two Schiff bases, the non-linear multiple regressions were obtained by B3LYP/6-311G method. The results of this calculation are shown in Table 6.

$$E_{cal}\,\% = \frac{(A+B\times E_{HOMO}+C\times E_{LUMO}+D\times \mu)C_i}{1+(A+B\times E_{HOMO}+C\times E_{LUMO}+D\times \mu)C_i}\times 100 \quad (9)$$

The calculated efficiencies (E_{cal}%) from the eq 9 at different concentrations of these compounds show good correlations to experimental efficiencies (E_{exp}%) with correlation coefficients R^2= 0.89 for NBPA and R^2 = 0.91 for NCMBPA [67]. The plot of the experimental and the calculated inhibition efficiency (from COSMO method) for NBPA and NCMBPA compounds were presented in Fig. 8.The similar plots were obtained for the other methods (not shown).

3.6. SEM analysis

The SEM images of copper specimens exposed to 6.0 M HCl for 3 h with and without 0.01M NBPA and NCMBPA are given in Fig. 9. It can be obviously observed from Fig. 8b that the surface morphology was severely corroded in the absence of inhibitors. However, in the presence of inhibitors, the destruction of copper surfaces is clearly reduced and even the polishing lines can be observed (Fig. 9c and d). This observation clearly proves that NBPA and NCMBPA can show good inhibiting ability on copper surface. The inhibitors may form protective films adsorbed on metal surface, resulting in a decrease in the contact between copper and the corrosive solution.

4. Conclusion

The studied two N- Benzylidene derivative compounds are professional inhibitors for the corrosion of copper in 6.0 M hydrochloric acid solutions. Polarization curves show that corrosion

potentials shift toward the anodic region at presence of the examined two N- Benzylidene derivative compounds.

The results of impedance demonstrate that as the additive concentration is increased the polarization resistance increases. Adsorption of the inhibitor molecules onto the copper surface follow by the Langmuir isotherm. The activation parameters of corrosion process such as activation energy (E_a), activation enthalpy (ΔH^*) and activation entropy (ΔS^*), are calculated from the dependence of corrosion rates on the temperature.

Through the quantum calculation methods used, the B3LYP/6-311G** and COSMO methods shows that the best correlation for some of the parameters studied and experimental results. The fact that inhibition efficiencies increase when the E_{LUMO} decrease shows that feedback bonds form between the Schiff bases and copper surface. Quantum chemical calculations were further applied to explain the experimental results[45,68].

Acknowledgments

We are grateful to University of Kashan for supporting this work with Grant 256450-12.

Reference

[1] G. Tansug, T. Tuken, E.S. Giray, G. Fındıkkıran, G. Sıg ırcık, O. Demirkol, M. Erbil, *Corros. Sci.* 84 (2014) 21-29.

[2] M.M. Antonijevic, B.M.B. Petrovic, *Electrochem. Sci*. 3 (2008) 1–28.

[3] M.M. Antonijevic, S.M. Milic, M.B. Petrovic, *Corros. Sci*. 51 (2009) 1228–1237.

[4] S.Sudheer, M.A. Quraishi, *Corros. Sci*. 70 (2013) 161–169.

[5] M. Scendo, *Corros. Sci*, 47 (2005) 1738–1749.

[6] E. S.Zocs, Gy.Vastag, A. Shaban, E. Kalman, *Corros. Sci*, 47 (2005) 893–908.

[7] E.M. Sherif, Su-Moon Park, *Electrochim. Act* , 51 (2006), 4665-4671

[8] M. Behpour, S. M. Ghoreishi, M. Khayat Kashani, N. Soltani, mater, *Corros.Sci*, 53 (2011) 2489-2501.

[9] M. Behpour, S. M. Ghoreishi, N. Soltani, M. Salavati-Niasari, *Corros. Sci*, 51 (2009) 1073-1089.

[10] S. Li, H. Ma, S. Lie, R. Yu, S. Chen, D.Liu, *Corros*, 54 (1998), 947-953.

[11] T. T. Qin, J. Li, H.Q. Luo, M.Li, N.B. Li, *Corros.Sci*, 53 (2011) 1072-1078.

[12] M. Behpour, S. M. Ghoreishi, N.Soltani, M. Salavati-Niasari, *Corros.Sci*,52.(2010), 4046-4057.

[13] M.G. Fontana and N. D. Greece, McGraw-Hill, *Corros. Eng*, New York, (1986).

[14] Y. Abboud, A. Abourriche, T. Saffaj, M. Berrada, M. Charrouf, A. Bennamara, N. Al Himidi, H. Hannache, Mater.*Chem. Phy*,105(2007)1-142.

[15] M. Lebrini, M. Lagren´ee, H. Vezin, L. Gengembre. F.Bentis, *Corros. Sci*. 47 (2005) 485.

[16] I. Dehri, M. Ozcan, Mater, *Chem. Phys*, 98 (2006) 316.

[17] F. Zucchi, G. Trabanelli, M. Fonsati, *Corros. Sci*, 38 (1996) 2019–2029.

[18] M. Finšgar, *Corros. Sci*, 77 (2013) 350– 359.

[19] H.O. Curkovic, E. Stupnisek-Lisac, H. Takenouti, *Corros. Sci*, 51 (2009) 2342–2348.

[20] R. Vera, F. Bastidas, M. Villarroel, A. Oliva, A. Molinari, D. Ramirez, R. del Rio, *Corros. Sci*, 50 (2008) 729–736.

[21] F. Zucchi, G. Trabanelli, C. Monticelli, *Corros. Sci*, 38 (1996) 147–154.

[22] K.F. Khaled, Mater, *Chem. Phys*, 125 (2011) 427–433.

[23] D. Gopi, K.M. Govindaraju, V.C.A. Prakash, D.M.A. Sakila, L. Kavitha, *Corros. Sci*, 51 (2009) 2259–2265.

[24] G. Kear, B.D. Barker, F.C. Walsh, *Corros. Sci*, 46 (2004) 109–135.

[25] M. Scendo, *Corros. Sci*, 50 (2008) 1584–1592.

[26] F. Rosalbino, R. Carlini, F. Soggia, G. Zanicchi, G. Scavino, *Corros. Sci*, 58 (2012) 139–144.

[27] M.B. Valcarce, M. Vazquez, *Corros. Sci*, 52 (2010) 1413–1420.

[28] A. A. Farag, M.A. Hegazy, *Corros. Sci*, 74 (2013) 168–177.

[29] M. Gopiraman, N. Selvakumaran, D. Kesavan, R. Karvembu, *Prog. Org. Coat*. 73 (2012) 104–111.

[30] S.T. Zhang, Z.H. Tao, W.H. Li, B.R. Hou, *Appl. Surf. Sci*, 255 (2009) 6757–6763.

[31] M. Lashgari, M Arshadi, S. Miandari, *Electrochim. Acta*, 55 (2010) 6058–6063.

[32] A.Yuce, G.Kardas, *Corros. Sci*, 58 (2012) 86– 94.

[33] Issaadi, T. Douadi, A. Zouaoui, S. Chafaa, M.A. Khan, G. Bouet, *Corros. Sci*, 53 (2011) 1484 1488.

[34] M.A. Migahed, Ahmed A. Farag, S.M. Elsaed, R. Kamal, H. Abd El-bary, *Chem. Eng. Commun*, 199 (2012) 1335–1356.

[35] I. Ahamad, R. Prasad, M.A. Quraishi, *Mater. Chem. Phys*, 124 (2010) 1155–1165.

[36] H.A. Mohamed, A.A. Farag, B.M. Badran, *J. Appl. Poly. Sci*, 117 (2010) 1270–1278.

[37] Serpil. Safak, Berrin. Duran, Aysel. Yurt, Gulsen. Turkoglu, *Corros. Sci*, 54 (2012) 251– 259.

[38] A.A. Farag, M.R. Noor El-Din, *Corros. Sci*, 64 (2012) 174–183.

[39] K.C. Emregul, O. Atakol, *Mater. Chem. Phys*, 83 (2004) 373– 379.

[40] I.B. Obot, N.O. Obi-Egbedi, S.A. Umoren, *Corros. Sci*, 51 (2009) 276–282.

[41] H. Naeimi, Z. S. Nazifi. Bull. *Chem. Soc. Ethiop*, 27 (2013) 143-149.

[42] A. Klamt, G. Schuurmann. *J. Chem. Soc. Perkin Trans*, 2 (1993) 799-805.

[43] W.Deng , P. Lin, Q. Li, G. Mob. Corros.Sci, 74 (2013) 44–49

[44] S.S. de Assunção Araújo Pereira, M.M. Pegas, T.L. Fernández, M. Magalhães, T.G. Schöntag, D.C. Lago, L.F. de Senna, E. D'Elia, *Corros. Sci*, 65 (2012) 360–366.

[45] M. Behpour, S.M. Ghroreishi, N. Soltani, M. Salavati-Niasari, M. Hamadanian, A. Gandomi, *Corros. Sci*, 50 (2008) 2172–2181.

[46] K.F. Khaled, *Mater. Chem. Phys*, 112 (2008), 104-111.

[47] M.Behpour, N.Mohammadi, E.Alian, *Journal of Iron and Steel Research International*, 21 (2014) 121-124.

[48] L. Li, Q. Qu, W. Bai, F.C. Yang, Y.J. Chen, S.W. Zhang, Z.T. Ding, *Corros. Sci*, 59 (2012) 249–257.

[49] A.Y. Musa, R.T.T. Jalgham, A.B. Mohamad, *Corros. Sci*, 56 (2012) 176–183.

[50] A. Popova, M. Christov, J. Univ. *Chem. Technol. Metall*, 43 (2008) 37–47.

[51] A. Yurt, G. Bereket, A. Kivrak, A. Balaban, B. Erk, *J. Appl. Electrochem*, 35 (2005) 1025–1032.

[52] A.M. Fekry, R.R. Mohamed, *Electrochim. Acta*, 55 (2010) 1933–1939.

[53] V.R. Saliyan, A.V. Adhikari, *Corros. Sci*, 50 (2008) 55–61.

[54] L.M. Vracar, D.M. Drazic , *Corros. Sci*, 44 (2002) 1669–1680.

[55] J. Alijourani, K. Raeissi, M.A. Golozar, *Corros. Sci*, 51 (2009) 1836–1843.

[56] D. Daoud, T. Douadi, S. Issaadi, S. Chafaa, *Corros Sci*, 79 (2014) 50–58.

[57] W. Li, X. Zhao, F. Liu, B. Hou, *Corros. Sci*, 50 (2008) 3261–3266.

[58] L. Larabi, O. Benali, Y. Harek, *Mater. Lett*, 61(2007) 3287-3293.

[59] A. Popova, E. Sokolova, S. Raicheva, M. Christov, *Corros. Sci*, 45 (2003) 331-345.

[60] T. Szauer, A. Brandt, *Electrochim. Acta*, 26 (1981) 1209.

[61] M. Bouklah, N. Benchat, B. Hammouti, A. Aouniti, S. Kertit, *Mater. Lett*, 60 (2006)2840-2843.

[62] E. A. Noor, A.H. Al-Moubaraki, *Mater. Chem. Phys*, 110 (2008) 145-154.

[63] M. Finsgar, A. Lesar, A. Kokalj, I. Milosev, Electrochim. Acta 53 (2008) 8287–8297.

[64] H. Ju, Z. Kai, Li. Y.*Corros. Sci*. 50 (2008) 865–871.

[65] G. Gece.*Corros. Sci*. 50 (2008) 2981-2992.

[66] A. Kokalj. *Electrochim. Acta* 56 (2010) 745-755.

[67] A. Kokalj, S. Peljhan, M. Fins gar, I. Milosev. *J. Am. Chem. Soc*. 132 (2010) 16657–16668.

[68] H. Ashassi-Sorkhabi, B. Shaabani, D. Seifzadeh. *Appl. Surf. Sci*. 239 (2005) 154.

[69] J.Tomasi, B.Mennucci, R.Cammi. Chem. Rev. 105(2005): 2999-3094.

[70] M.Nadia Rega, G.Scalmani, V.Barone. J. Comput. Chem. 24(2003): 669-681.

Figure captions

Fig. 1. The chemical structure of the investigated Schiff bases

Fig. 2. The Nyquist plots of copper in hydrochloric acid 6.0 M with the various concentrations of: (a) NBPA, (b) NCMBPA

Fig. 3. Equivalent circuit model of impedance spectra in (a) Blank, (b) The different concentration of inhibitors

Fig. 4. Polarization curves for copper in hydrochloric acid 6.0 M solution with the (a) NBPA, (b) NCMBPA, in different concentrations

Fig. 5. The Langmuir isotherm for adsorption of NBPA and NCMBPA on the copper surface

Fig. 6. The plots of Ln (i_{corr}/T) vs. 1000/T for copper in hydrochloric acid 6.0 M in the absence and presence of 0.01M of inhibitors

Fig.7. The plots of Ln (i_{corr}) vs. 1000/*T* for copper in hydrochloric acid 6.0 M in the absence and presence of 0.01M of inhibitors

Fig. 8. The correlation between experimental inhibition efficiency and calculated inhibition efficiency obtained from COSMO method.

Fig. 9. The SEM images of the copper surface after 3 h immersion period (a) before corrosion, (b) 6.0 M HCl, (c) 6.0 M HCl + 0.01M NBPA, (d) 6.0 M HCl + 0.01M NCMBPA,

Table captions

Table.1. The results of the impedance spectra for copper in the absence and presence of various Concentrations of inhibitors in hydrochloric acid 6.0 M at 25 ºC

Table.2. Electrochemical kinetic parameters obtained by Tafel polarization technique for copper in the absence and presence of various concentrations of inhibitors in hydrochloric acid 6.0 M at 25 ºC

Table.3. ΔG_{ads}, E_a, ΔH^*, ΔS^*, of dissolution reaction of copper in hydrochloric acid 6.0 M solution

Table.4. Polarization parameters and corresponding inhibition efficiency for the corrosion of the copper in hydrochloric acid 6.0 M without and with addition of 0.01 M the inhibitors at different temperatures

Table.5. Quantum chemical parameters of used Schiff bases obtained from quantum method

Table 6. Coefficients of Eq (9) obtained from quantum chemical parameters for applied quantum method.

Table.1. The results of the impedance spectra for copper in the absence and presence of various Concentrations of inhibitors in hydrochloric acid 6.0 M at 25 ºC

Inhibitor	Concentration (M)	R_s (Ω cm^2)	R_{ct} (Ω cm^2)	Y_0 (μF cm^{-2})	n	η%
Blank	-	3.3±0.041	98.6±0.10			
NBPA	5×10^{-4}	2.2±0.059	603.89±0.59	$0.001860\pm0.6\times10^{-6}$	0.49±0.0053	84.0±0.8
	1×10^{-3}	2.3±0.013	687.77±1.5	$0.001060\pm0.6\times10^{-6}$	0.52±0.0059	86.0±1.2
	5×10^{-3}	2.0±0.019	734.19±2.3	$0.000974\pm0.3\times10^{-6}$	0.55±0.0059	87.0±0.9
	1×10^{-2}	2.0±0.039	847.44±3.6	$0.000647\pm0.7\times10^{-6}$	0.56±0.0059	88.0±1
NCMBPA	5×10^{-4}	1.3±0.059	580.20±1.5	$0.00270\pm0.6\times10^{-6}$	0.48±0.0053	83.0±0.8
	1×10^{-3}	1.5±0.059	681.00±2.1	$0.00112\pm0.6\times10^{-6}$	0.54±0.0059	86.0±1.1
	5×10^{-3}	1.8±0.053	866.90±3.4	$0.00110\pm0.6\times10^{-6}$	0.54±0.0059	89.0±0.9
	1×10^{-2}	2.1±0.053	1257.8±9.6	$0.00068\pm0.7\times10^{-6}$	0.55±0.0059	92.0±1

Table.2. Electrochemical kinetic parameters obtained by Tafel polarization technique for copper in the absence and presence of various concentrations of inhibitors in hydrochloric acid 6.0 M at 25 ^{o}C

Inhibitor	Concentration (M)	b_a (mV dec $^{-1}$)	$-b_c$ (mV dec $^{-1}$)	-E vs Ag/Agcl(3 M Cl^-) (mV)	Icorr (µA cm^{-2})	η %
Blank	-	131.2±1	120.4±1	482.1±3	230.1±0.07	-
NBPA	5×10^{-4}	223.3±1	106.5±2	201.9±2	47.3±0.04	79.0±0.6
	1×10^{-3}	225.6±2	107.4±1	198.4±1	45.4±0.05	80.0±0.2
	5×10^{-3}	195.1±1	102.3±4	197.7±1	36.3±0.01	84.0±0.2
	1×10^{-2}	171.0±2	102.4±1	201.7±2	32.6±0.06	86.0±0.5
NCMBPA	5×10^{-4}	212.4±1	124.9±1	215.6±1	62.4±0.05	73.0±0.1
	1×10^{-3}	133.5±3	100.0±3	205.6±3	33.7±0.02	85.0±0.3
	5×10^{-3}	123.1±2	98.7±1	204.2±1	28.5±0.02	88.0±0.1
	1×10^{-2}	83.4±1	59.8±1	185.2±1	16.8±0.01	93.0±0.9

Table.3. ΔG_{ads}, E_a, ΔH^*, ΔS^*, of dissolution reaction of copper in hydrochloric acid 6 M solution

Inhibitor	K_{ads} ($\times 10^3$)	R^2	ΔG_{ads} (KJ mol^{-1})	E_a (KJ mol^{-1})	ΔH^*_{ads} (KJ mol^{-1})	ΔS^*_{ads} (J $mol^{-1}k^{-1}$)
Blank	-	-	-	28.18	25.7	-128.7
NBPA	20	0.99	-33.7	32.18	26.3	-119.2
NCBMPA	12.5	0.99	-32.6	36.86	35.2	-102.3

Table.4. Polarization parameters and corresponding inhibition efficiency for the corrosion of the copper in hydrochloric acid 6 M without and with addition of 0.01 M the inhibitors at different temperatures

Inhibitor	Temperature (^{0}C)	b_a (mV dec $^{-1}$)	$-b_c$ (mV dec $^{-1}$)	-E vs Ag/Agcl(3 M Cl^-) (mV)	I_{corr} (µA cm^{-2})	η%
Blank	35	123.1±1	167.5±2	451.0±1	202.2±0.07	-
	45	109.6±2	104.7±1	482.8±1	213.1±0.07	-
	55	153.9±2	198.5±1	453.5±1	260.6±0.04	-
	65	130.9±1	204.8±3	458.5±2	310.0±03	-
NBPA	35	159.8±1	95.80±2	184.8±1	42.60±0.04	79.0±1.2
	45	64.90±3	318.0±2	423.0±2	64.20±0.01	70.0±1.4
	55	81.00±2	98.30±1	440.2±3	90.90±0.05	65.0±0.8
	65	123.9±1	249.4±1	430.2±1	120.8±0.07	61.0±1.6
NCBMPA	35	97.90±1	77.00±1	201.4±1	31.40±0.03	84.0±1.3
	45	107.3±2	138.1±3	337.9±2	56.40±0.02	74.0±1.1
	55	46.60±3	71.90±1	446.3±1	80.70±0.03	69.0±0.5

Table.5. Quantum chemical parameters of used Schiff bases obtained from quantum method

method	Parameters	Inhibitor	
		NBPA	NCMBPA
B3LYP /6- 311G**	E_{Homo}(ev)	-0.2362	-0.2343
	E_{Lumo}(ev)	-0.0771	-0.0819
	ΔE(ev)	0.1591	0.1524
	μ(D)	3.4076	4.5691`
PCM	E_{Homo}(ev)	-0.2362	-0.2343
	E_{Lumo}(ev)	-0.0771	-0.0819
	ΔE(ev)	0.1591	0.1524
	μ(D)	3.4076	4.5691
CPCM	E_{Homo}(ev)	-0.2398	-0.2376
	E_{Lumo}(ev)	-0.0811	-0.0848
	ΔE(ev)	0.1587	0.1528
	μ(D)	4.0109	4.6504

Table 6. Coefficients of Eq (9) obtained from quantum chemical parameters for applied quantum methods.

	state*	Coefficient			
		A	B	C	D
B3LYP /6-311G**	I	19851.16	27409.14	1013032.35	730.65
	II	21940.67	26902.70	100903.37	65.54
PCM	I	21938.22	26891.24	100908.27	65.58
CPCM	I	22870.07	26665.90	100850.15	66.50

* In state I, the D coefficient is equal zero

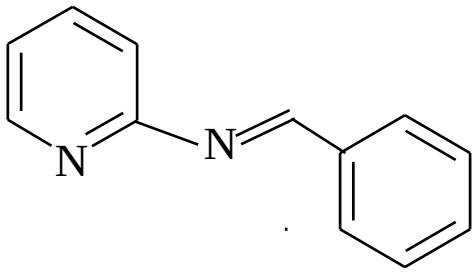

E-N-benzylidenepyridin-2-amine

(NBPA)

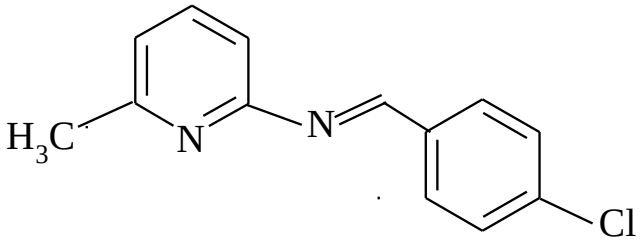

N-(4-choloromethylbenzylidene) Pyridin – 2 amine

(NCMBPA)

Fig. 1. The chemical structure of the investigated Schiff bases.

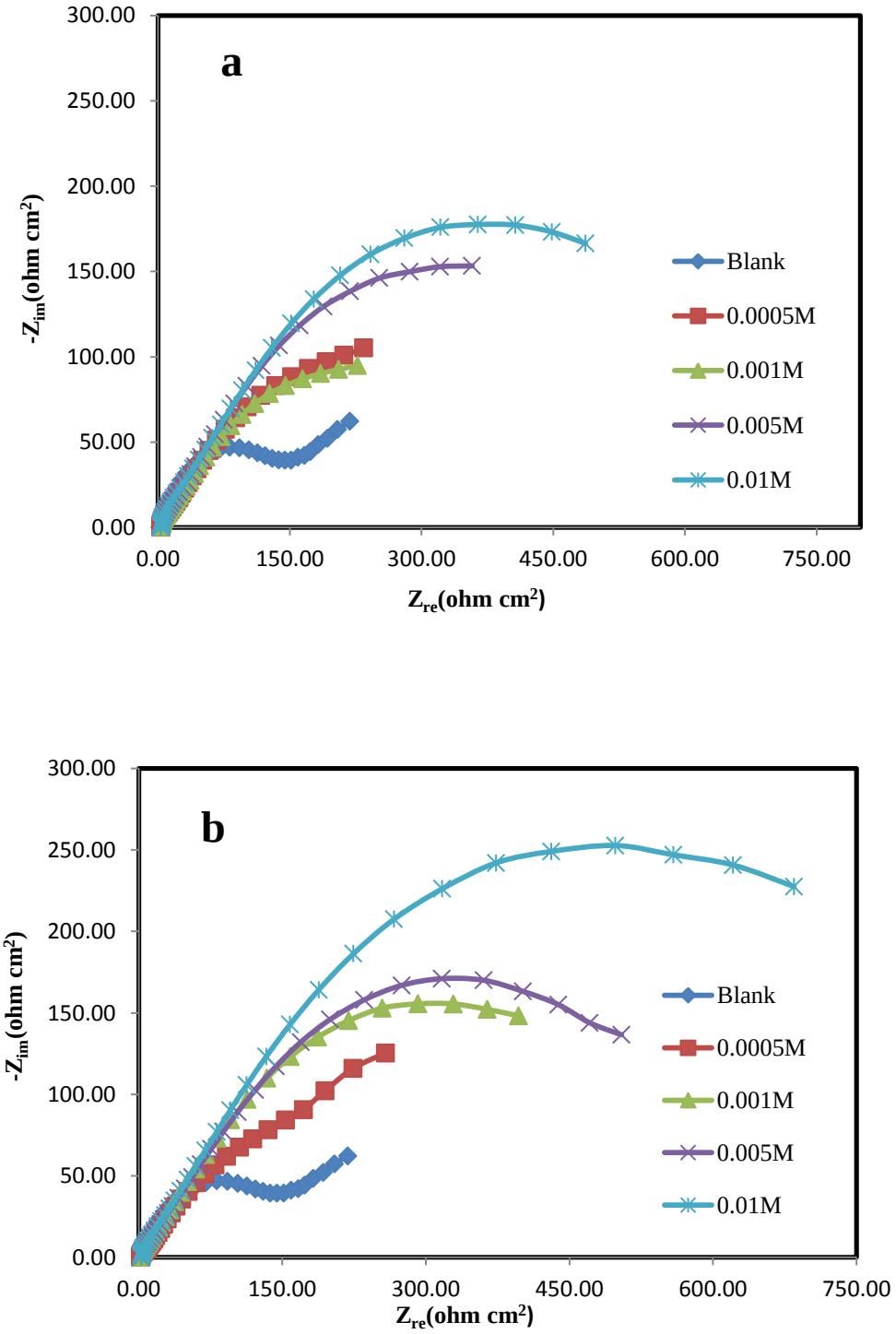

Fig. 2. The Nyquist plots of copper in hydrochloric acid 6M with the various concentrations of:

(a) NBPA, (b) NCMBPA.

(a)

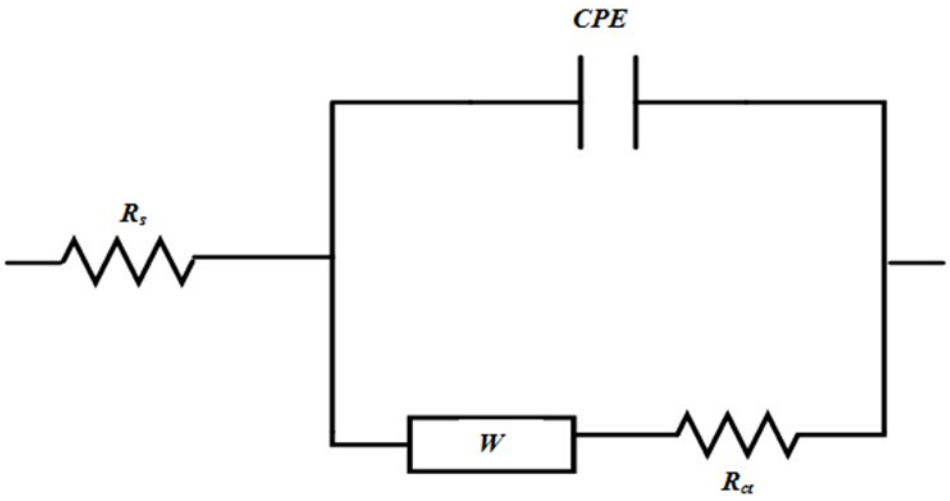

(b)

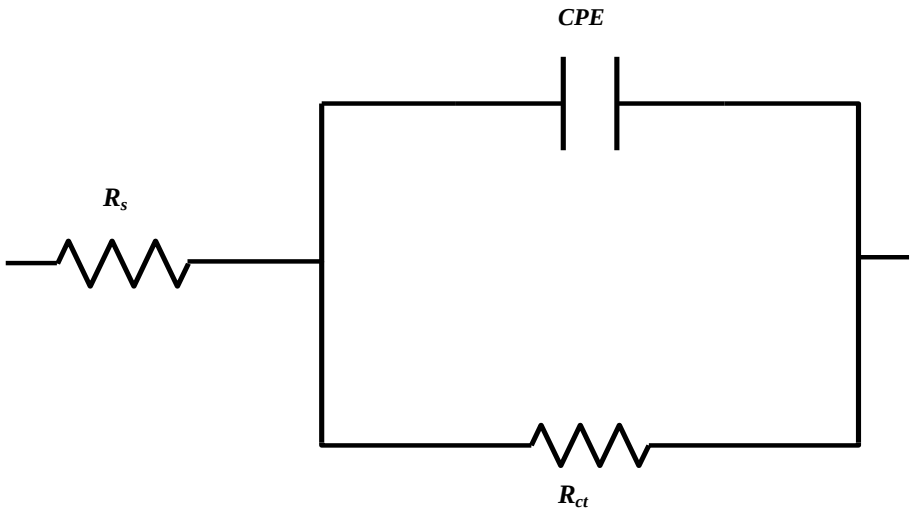

Fig. 3. Equivalent circuit model of impedance spectra in (a) Blank , (b) The different concentration of inhibitors.

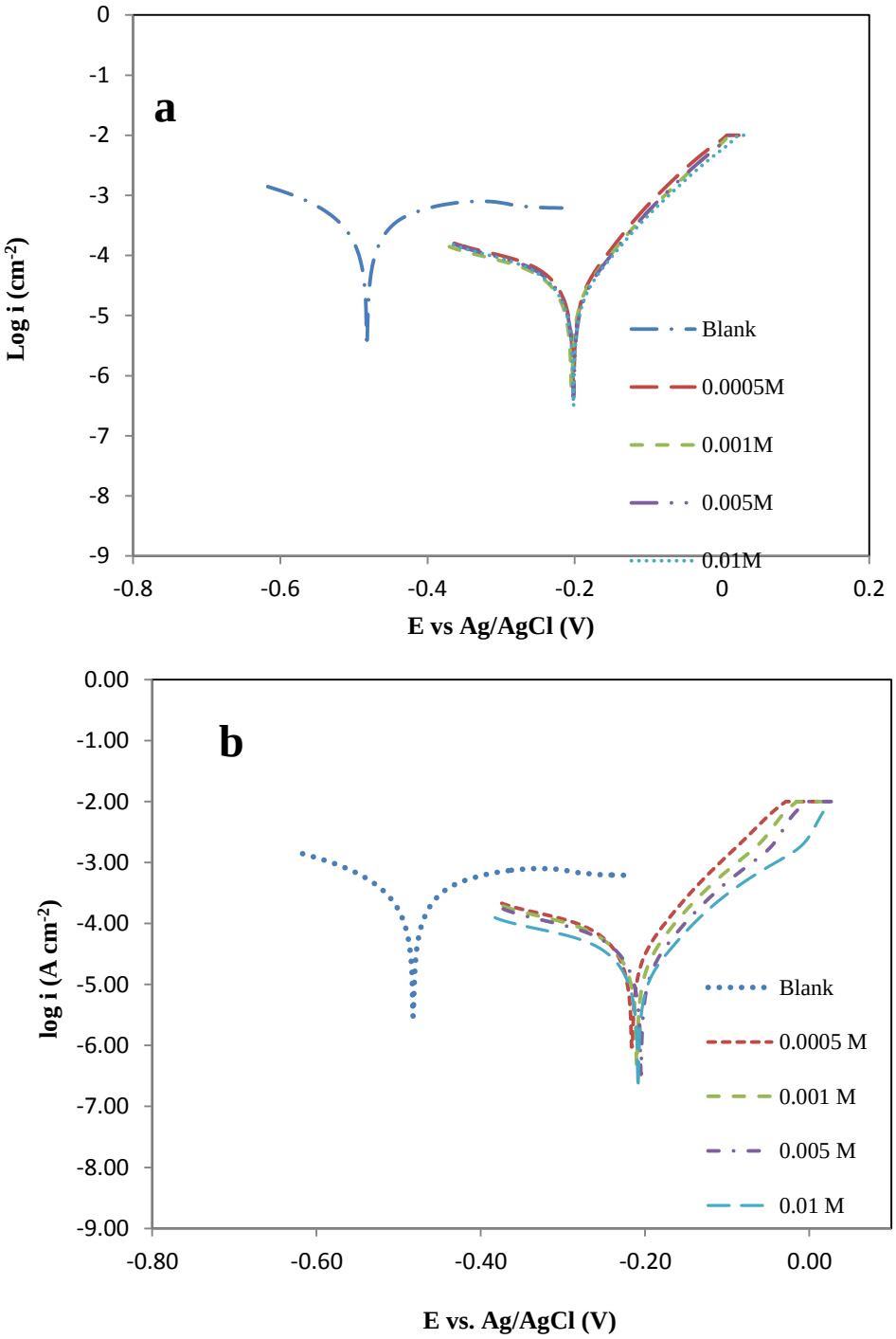

Fig. 4. Polarization curves for copper in hydrochloric acid 6.0 M solution with the (a) NBPA, (b) NCMBPA, in different concentrations.

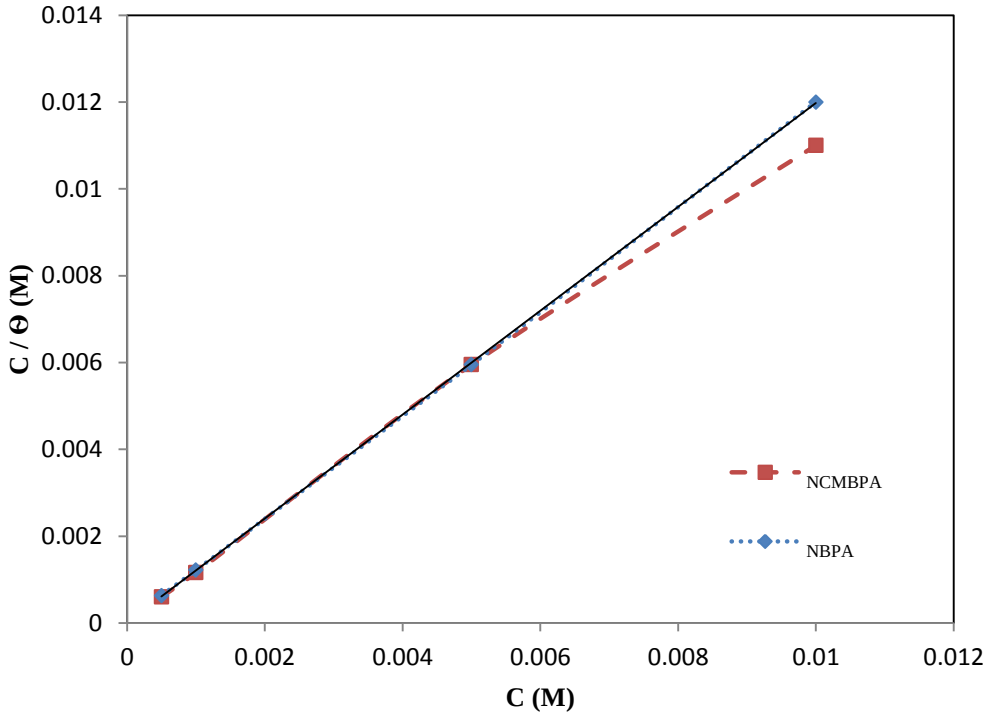

Fig. 5. The Langmuir isotherm for adsorption of NBPA and NCMBPA on the copper surface.

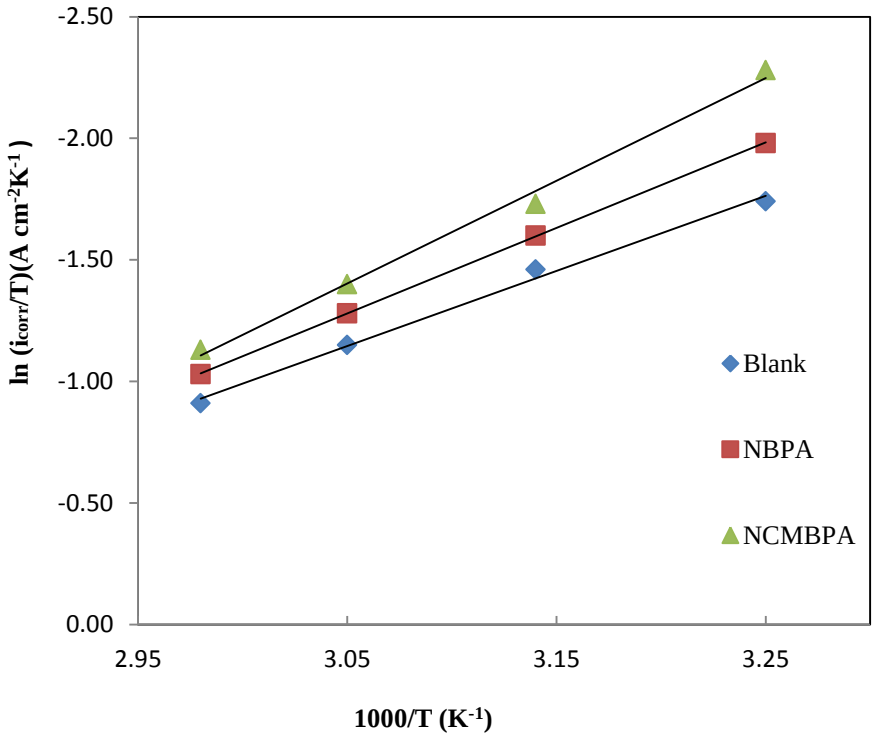

Fig. 6. The plots of Ln (i_{corr}/T) vs. 1000/T for copper in hydrochloric acid 6.0 M in the absence and presence of 0.01M of inhibitors.

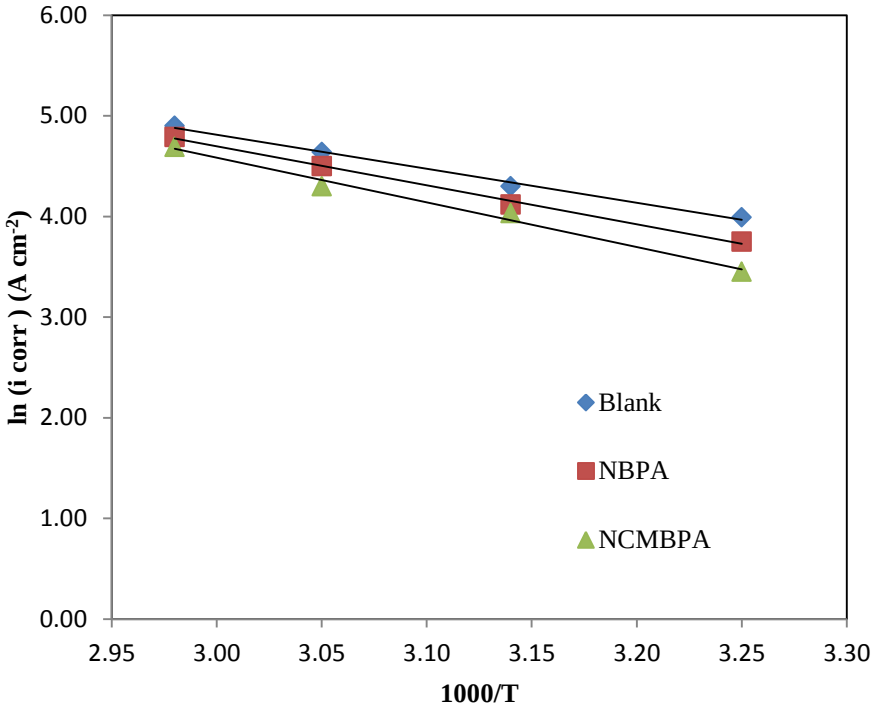

Fig.7. The plots of Ln (i_{corr}) vs. 1000/T for copper in hydrochloric acid 6.0 M in the absence and presence of 0.01M of inhibitors.

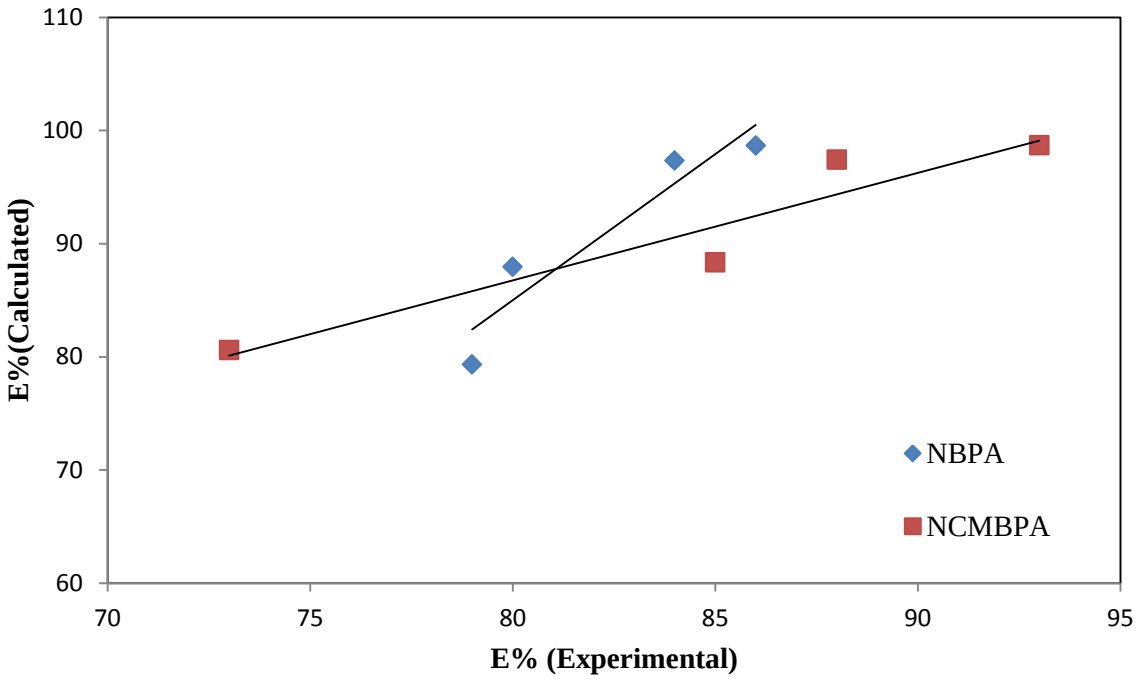

Fig. 8. Correlation between experimental inhibition efficiency and calculated inhibition efficiency obtained from COSMO method.

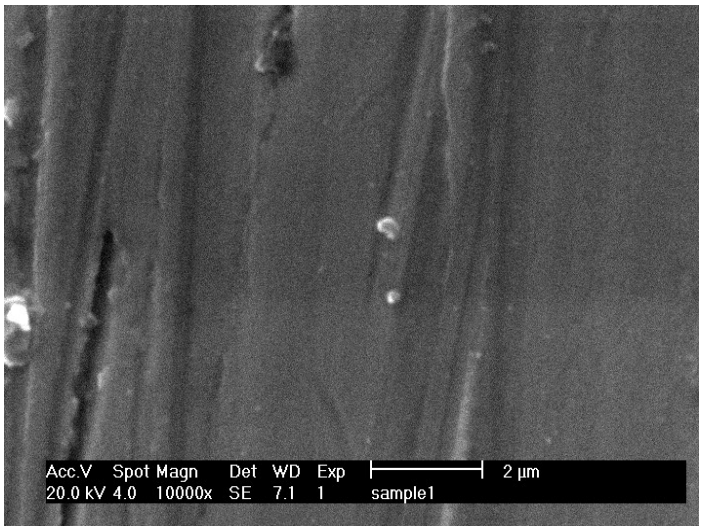

(a)

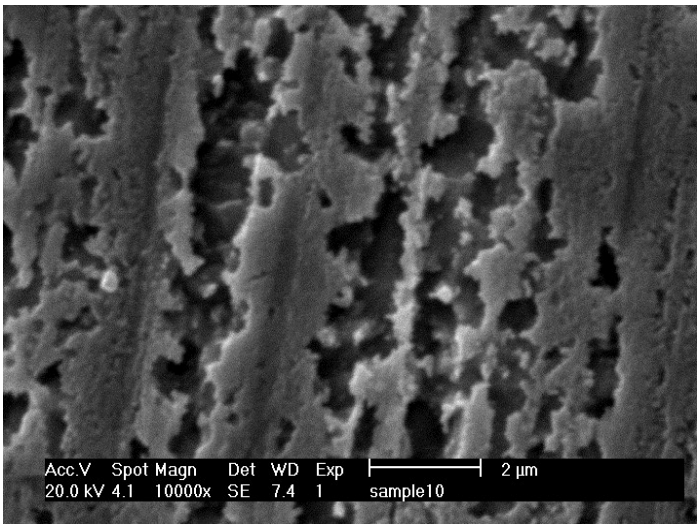

(b)

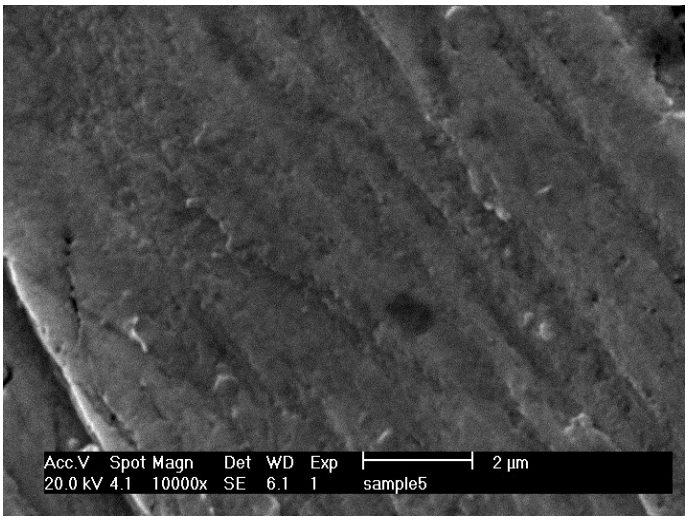

(c)

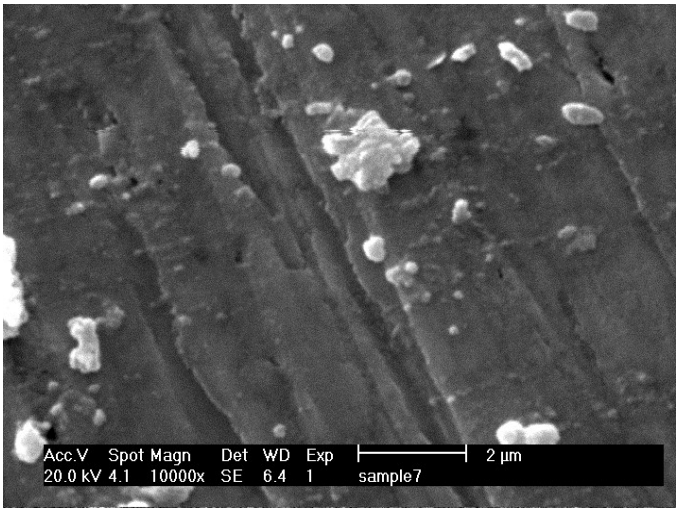

(d)

Fig.9. The SEM images of the copper surface after 3 h immersion period (a) before corrosion, (b) 6.0 M HCl, (c) 6.0 M HCl + 0.01M NBPA, (d) 6.0 M HCl + 0.01M NCMBPA,